SCIENCE CHINA Materials

LETTERS

mater.scichina.com link.springer.com

Published online 29 November 2018 | https://doi.org/10.1007/s40843-018-9375-x

Sci China Mater 2019, 62(6): 907–912

Anomalous low-temperature transport property of oxygen containing high-entropy Ti-Zr-Hf-Cu-Ni metallic glass thin films

Shaofan Zhao[1*], Pengfei Wang[1], Xiang Cheng[1], Yingqi Zhang[2], Zhuoqun Wen[1], Qi Zhang[1], Ke-Fu Yao[2], Na Chen[2*] and Wei-Hua Wang[3]

Lacking structural periodicity of long-range order induces unusual physical properties in metallic glasses (MGs) [1–3]. Specifically, the low-temperature electron transport behavior of MGs has triggered fundamental interest in solid-state physics [4,5]. MGs exist as strong scattering systems since their electron mean free paths are comparable to the average interatomic distances [4–6]. The temperature coefficient of resistivity (TCR, defined as $\alpha = (1/\rho)(\partial\rho/\partial T)$) in these systems can be positive or negative depending on their Fermi level positions [7]. At low temperatures, metal-insulator transition could occur in MGs owing to either disorder-induced Anderson localization or electron-electron interactions [8–10]. Moreover, MGs have many configurational states associated with different structural relaxation processes as described in the concept of potential energy landscape [11–13]. The supercooled liquid experiences various inherent structures corresponding to different energy minima of potential energy landscape before it becomes stuck into a single minimum at the glass transition [14]. During cooling, configurational entropy is known to be a key parameter to determine the size of cooperatively rearranging regions that manifests both dynamic and structural heterogeneity [14–16]. High configurational entropy has been proposed to enhance structural homogeneity and degree of disorder of MGs [17–22], leading to high room-temperature electrical resistivity in high entropy MGs (HEMGs) [23].

Oxygen is detrimental to the glass forming ability (GFA) of MGs; however, very limited oxygen might be effective in improving the GFA of Fe-based MG [24] and enhancing the yield strength of Zr-based MG [25]. The structures and properties could be obviously affected or adjusted by oxygen addition. In addition, incorporating oxygen into the MGs could make the structure of MGs more disordered [26,27]. This may further enhance the electron-electron interaction in disordered solids and lead to interesting low-temperature electron transport behaviors. However, systematic research on the electrical properties of HEMGs is still lacking, particularly for the low-temperature electrical behavior, which is closely related to its electronic structure and reflects its glass nature. In this study, we focused on low-temperature electrical and magnetoelectric properties of oxygen incorporated Ti-Zr-Hf-Cu-Ni HEMG thin films (O-HEMG). An anomalous electric resistivity was found in the HEMG oxide below 8 K.

The HEMG films were deposited on the glass substrates from a $Ti_{20}Zr_{20}Hf_{20}Cu_{20}Ni_{20}$ (at.%) high entropy metallic target by a direct-current (DC) magnetron sputtering system. We used pure argon, gas mixture with the volume concentration of 99.85 vol.% or 99.25 vol.% for argon and 0.15 vol.% or 0.75 vol.% for oxygen with working pressure of 0.6 Pa. During sputtering, a Hall bar template was attached on the Si substrates. Then, the deposited HEMG films and O-HEMG have a mesa structure in shape of the Hall bar with a typical size of 1.067 mm in width and 6.667 mm in length. The thickness of the HEMG films and O-HEMG was measured by a step profiler. The chemical composition of the deposited O-HEMG was examined by an energy dispersive spectrometer (EDS). The composition of HEMG film is $Zr_{23.4}Ni_{22.9}Cu_{18.5}Hf_{17.7}Ti_{17.5}$, while that of the O-HEMG turned out to be $O_{10.2}Ni_{24.0}Cu_{22.3}Ti_{16.5}Hf_{11.9}Zr_{15.1}$ and $O_{46.2}Cu_{14.5}Ni_{13.7}Zr_{9.9}$-

[1] Qian Xuesen Laboratory of Space Technology, Beijing 100094, China
[2] School of Materials Science and Engineering, Tsinghua University, Beijing 100084, China
[3] Institute of Physics, Chinese Academy of Sciences, Beijing 100190, China
[*] Corresponding authors (emails: zhaoshaofan@qxslab.cn (Zhao S); chennadm@mail.tsinghua.edu.cn (Chen N))

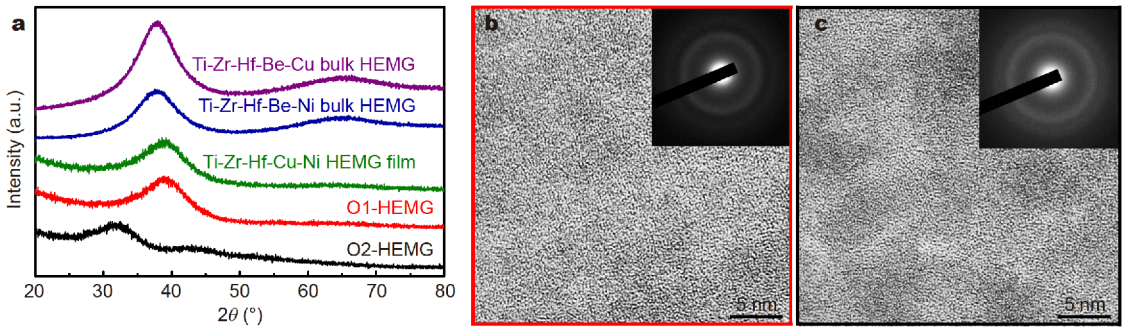

Figure 1 XRD patterns for bulk HEMGs, HEMG films and O-HEMG (a) and HRTEM images (b, c) for O-HEMG films. The insets in (b, c) are their corresponding SAED patterns.

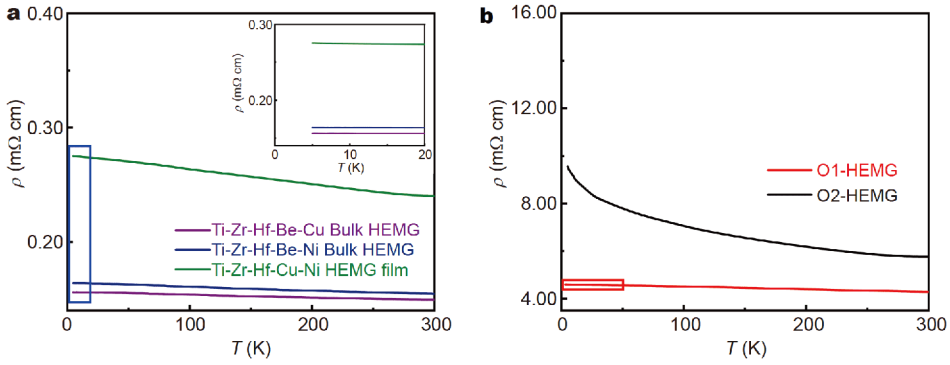

Figure 2 Electrical properties of bulk HEMGs, HEMG film (a) and O-HEMG (b). The inset is the enlargement of the part marked by the blue square in (a).

$Ti_{9.7}Hf_{6.0}$ (at.%), which are simplified as O1-HEMG and O2-HEMG, respectively. By comparison, $Ti_{20}Zr_{20}Hf_{20}Be_{20}Cu_{20}$ and $Ti_{20}Zr_{20}Hf_{20}Be_{20}Ni_{20}$ bulk HEMGs without oxygen were prepared by the Cu mold suction casting after alloying the metals of high purity. The cast bulk HEMG sheets were then processed into the same Hall bar shape by a wire-electrode cutting. The microstructure of O-HEMG films was characterized by a high-resolution transmission electron microscope (HRTEM) and an X-ray diffractometer. Temperature-dependent resistivity ranging from 5 to 300 K and magnetoresistivity (MR) of O1-HEMG were measured using a four-terminal probe technique with a Quantum Design physical property measurement system (PPMS). The components and chemical states of the films were analyzed by X-ray photoelectron spectroscopy (XPS) with mono-chromatized Al Kα excitation.

Fig. 1a shows the XRD patterns of the bulk HEMGs, HEMG film and O-HEMG and no sharp diffraction peaks corresponding to crystalline phases are observed, indicative of the formation of amorphous structure. Only O2-HEMG with high oxygen content exhibits two close peaks in its XRD pattern, while the O1-HEMG with low oxygen content presents only one broad peak. HRTEM images of O1-HEMG (Fig. 1b) and O2-HEMG (Fig. 1c) present maze-like pattern of highly disordered atomic arrangments. From the corresponding selected area electron diffraction (SAED) pattern of O2-HEMG as shown in the insets of Fig. 1c, two broad diffraction halo rings can be found, which are typical for oxide and in consistent with its XRD pattern in Fig. 1a. Particularly, it can be noticed that O1-HEMG, containing less oxygen, is still a single-phase MG from its XRD and SAED (the inset of Fig. 1b) patterns.

TCR of these MGs are shown in Fig. 2. The electrical resistivity of Ti-Zr-Hf-Be-Cu, Ti-Zr-Hf-Be-Ni bulk HEMGs and Ti-Zr-Hf-Cu-Ni HEMG film at room temperature are 0.150, 0.155 and 0.240 mΩ cm, showing a negative TCR between 5 to 300K. However, such negative temperature dependence of resistivity is frequently observed in MGs [28]. Mooij proposed that the negative TCR is directly related to the strong scattering and the

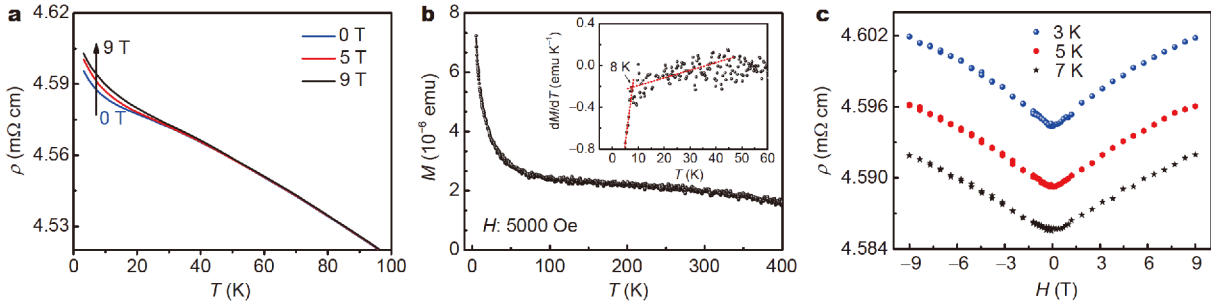

Figure 3 (a) Low-temperature electron transport properties of O1-HEMG under H up to 9 T . (b) M-T curve under H of 5000 Oe. The inset indicates the crossover temperature is ~8 K. (c) The resistivity of O1-HEMG under different H below 8 K.

relatively high resistivity, indicating the conductive electron mean free path is very small [4]. Owning to the strong scattering in HEMGs, the localization of conduction electrons leads to bound states, from which more electrons can be thermally excited with increasing temperature [4].

In Fig. 2b, oxygen incorporated HEMG films lead to a higher room-temperature resistivity of 4.29 and 5.77 mΩ cm, which are one order of magnitude higher than those of the HEMGs. More specifically, compared with the bulk HEMGs, the addition of oxygen changes the low-temperature resistivity behavior of O-HEMG. In the inset of Fig. 2a, the resistivity of bulk HEMGs shows a slight dependence on temperature below 20 K. As indicated in Fig. 2b, a slope divergence is obviously observed at low temperature for O2-HEMG. Same phenomenon can be also found below 8 K for O1-HEMG in Fig. 3a which is the enlarged view of the red rectangle region in Fig. 2b. This slope divergence indicates a transition of the conduction mechanism occurs at low temperatures for O-HEMG.

Although the low temperature dependence of the resistivity of O1-HEMG sample is different from those of both bulk HEMGs and HEMG film, its XRD pattern and HRTEM image confirm that O1-HEMG is still a single-phase MG. To understand the mechanism for its low-temperature electrical transport behavior, we further measured the temperature dependence of its resistivity under an external magnetic field (H). As shown in Fig. 3a, increasing H enhances its low-temperature resistivity, showing a positive MR effect. At relatively high temperatures, the resistivity-temperature curves with different external fields merge together and coincide with the one measured without H. This indicates that such positive MR effect is only observed at low temperature.

To probe the origin for the magnetotransport properties, the temperature dependence of its magnetization (M-T) was obtained as shown in Fig. 3b. It is evident that the sample is paramagnetic. Below the crossover temperature of ~8 K as indicated in the inset of Fig. 3b, the O1-HEMG sample shows an increased magnetization under an external field of 5,000 Oe. Correspondingly, the resistivity of the O1-HEMG increases with the external field below 8 K (Fig. 3c), exhibiting an obviously positive magnetoresistance effect.

For paramagnetic disordered metals or alloys, the correction to its conductivity in a magnetic field can be described as a sum of two terms as follow [29]:

$$\Delta\sigma(H,T) = \sigma(H,T) - \sigma(H=0,T=0) \quad (1)$$
$$= \Delta\sigma_1(T) + \Delta\sigma_2(H,T),$$

where the first correction term $\Delta\sigma_1(T)$ scales with $T^{1/2}$ mainly due to long-range Coulomb interaction, which is independent of an external magnetic field which is denoted by H and gives rise to an $E^{1/2}$ (E stands for energy) dependence of the density of states at Fermi energy; $\Delta\sigma_2$ (H,T) is field-dependent correction term and can be described as:

$$\Delta\sigma_2(H,T) = \sigma_2(H,T) - \sigma_2(H=0,T) \sim H^{1/2}. \quad (2)$$

Combining Equations (1) and (2), the resulting $\sigma(H, T)$ should be related with both $H^{1/2}$ and $T^{1/2}$. Note that this field dependence of $H^{1/2}$ is only valid when the Zeeman effect induced spin splitting energy of $g\mu_B H$ is larger than the thermal energy of $k_B T$. This means the $H^{1/2}$ dependence of the conductivity occurs at very low temperatures and in high magnetic fields.

The conductivity of the O1-HEMG has been correlated with T and H as shown in Fig. 4. Below 8 K, $\sigma(H,T)$ indeed has $T^{1/2}$ and $H^{1/2}$ dependence. Especially, the upper temperature limit for this $T^{1/2}$ dependence increases with H as shown in Fig. 4a, while the lower magnetic field limit for $H^{1/2}$ dependence increases with T (Fig. 4b). It is suggested that the thermal energy and magnetic interac-

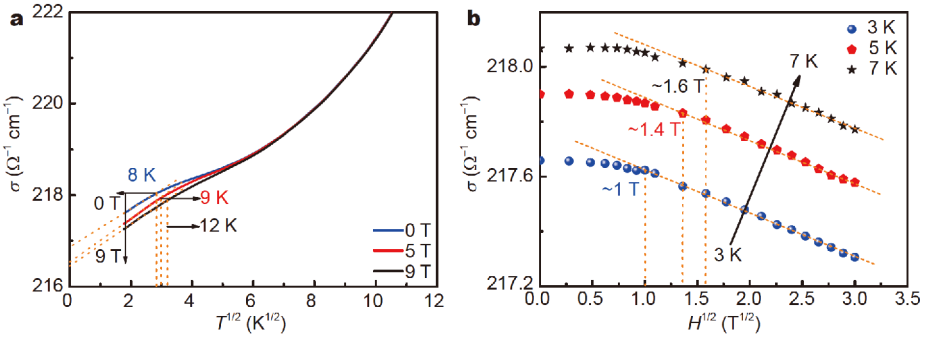

Figure 4 The $T^{1/2}$ (a) and $H^{1/2}$ (b) dependence of the conductivity of O1-HEMG.

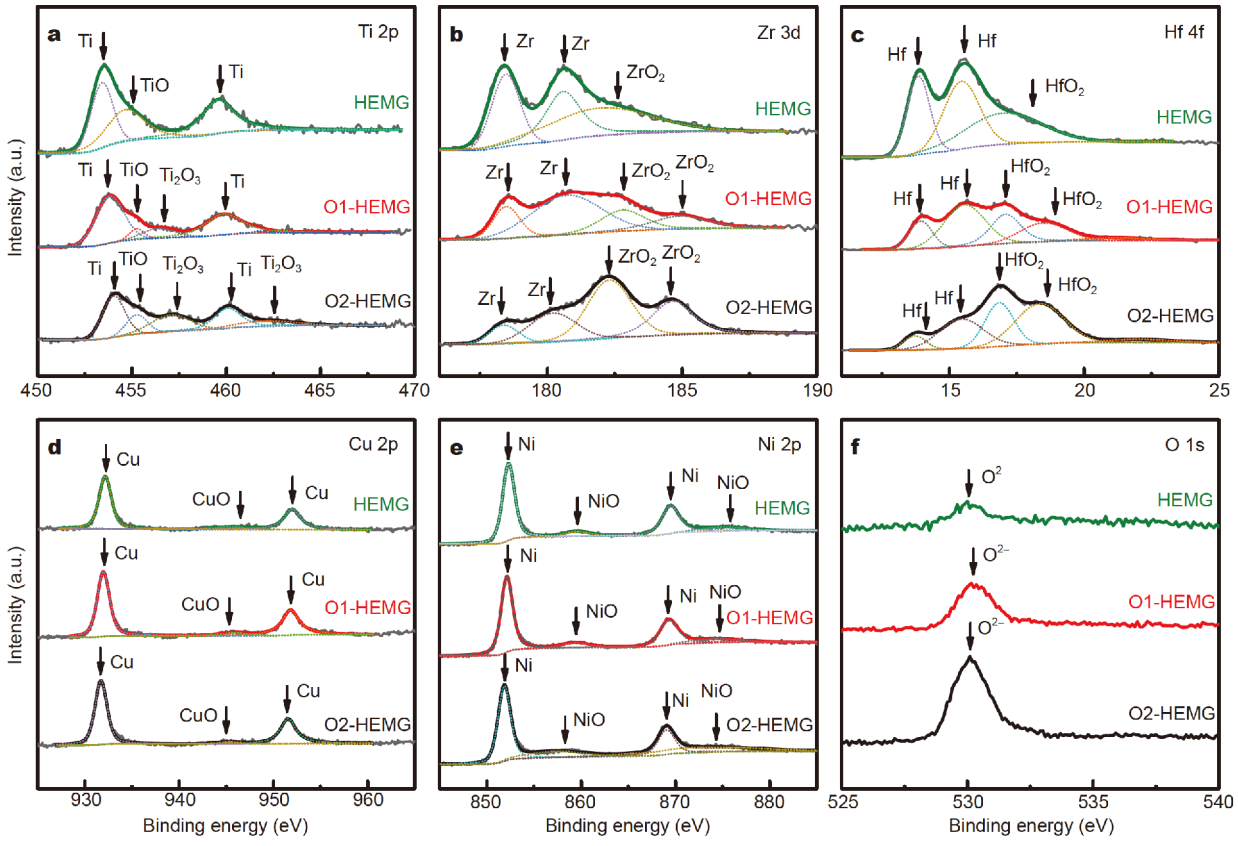

Figure 5 XPS spectra of Ti 2p (a), Zr 3d (b), Hf 4f (c), Cu 2p (d), Ni 2p (e) and O 1s (f) in the HEMG film, O1-HEMG and O2-HEMG.

tion effect couple each other to account for the electrical transport behavior of the O1-HEMG [30].

To elucidate the mechanism that how oxygen addition affects the structure of the HEMG film, XPS measurements were performed on the films with a depth of 60 nm from the surface. The XPS spectra are shown in Fig. 5, and all the spectra were calibrated by the C 1s spectrum corresponding to the contaminant hydrocarbon layer of the films. For HEMG film without oxygen addition, doublet peaks appear in each spectrum of Ti 2p, Zr 3d, Hf 4f, Cu 2p and Ni 2p, which originate from their zero-valence metallic states. Meanwhile, there also exist some weak peaks resulting from TiO, ZrO_2, HfO_2, CuO and NiO. These oxides might be caused by a very small fraction of oxygen contamination in the sputtering target. As for the spectra of O1-HEMG, the intensity of TiO,

ZrO_2, HfO_2 peaks became much stronger, and Ti_2O_3 peak appeared in the Ti 2p spectrum. With more oxygen addition in O_2-HEMG, ZrO_2 and HfO_2 peaks became dominant in Zr 3d and Hf 4f spectra. However, the spectra of Cu 2p and Ni 2p remained almost the same in the HEMG film and O-HEMG, because Cu and Ni have much lower affinity to oxygen than Ti, Zr and Hf [31]. Thus, during sputtering in a mixed gas environment, Ti, Zr and Hf, the elements which have relatively strong affinity to oxygen, firstly trapped oxygen atoms, leading to the formation of their oxides. In such case, it proves that oxygen addition can make the structure of HEMG more disordered.

Compared with the conventional bulk HEMGs and HEMG film without oxygen, O1-HEMG shows different low-temperature transport behavior. The $T^{1/2}$ and $H^{1/2}$ dependences of the conductivity of O1-HEMG emerge at low temperature and in high fields. The $T^{1/2}$ dependence is caused by the enhanced electron-electron Coulomb interaction independent of the external magnetic fields, while the $H^{1/2}$ dependence arises from the magnetic exchange interaction associated with spin splitting in high magnetic fields. In the conventional bulk HEMGs and HEMG film, the high electron carrier concentration screens the long-range electron-electron interaction. As a result, the $T^{1/2}$ dependence of the conductivity is absent in the bulk HEMGs and HEMG film as shown in the inset of Fig. 2a. The Ti-Zr-Hf-Cu-Ni HEMG only contains transition metals, which mainly comprises metallic bonds between these metals. The metallic bonds are known to be non-directional and non-saturated, which open a channel for inclusion of oxygen in a well-controlled manner. Thanks to the unique structural flexibility, oxygen involved in the Ti-Zr-Hf-Cu-Ni alloy helps localize some of the free electrons through forming the covalent bonds with the transition metals, e.g., Ti, Zr, and Hf in this alloy. Meanwhile, as mentioned above, the degree of disorder is also increased owing to the oxygen addition. The increased structural disorder strengthens the localization effect and enhances electron-electron interaction. They both contribute to the low-temperature transport behavior observed in the present O1-HEMG.

In conclusion, an anomalous low-temperature transport property showing $T^{1/2}$ and $H^{1/2}$ dependences of the conductivity at low temperature and in high magnetic fields is observed in oxygen containing HEMG films. The anomalous low-temperature transport is attributed to the enhancement of electron-electron Coulomb interaction and electron spin exchange interaction in the complicated and disordered glass. Our results indicate that inclusion of oxygen into HEMGs provides a new way to manipulate the low-temperature transport properties.

Received 7 November 2018; accepted 19 November 2018; published online 29 November 2018

1 Greer AL. Metallic glasses. Science, 1995, 267: 1947–1953
2 Inoue A. Stabilization of metallic supercooled liquid and bulk amorphous alloys. Acta Mater, 2000, 48: 279–306
3 Chen N, Louzguine DV, Ranganathan S, *et al.* Formation ranges of icosahedral, amorphous and crystalline phases in rapidly solidified Ti–Zr–Hf–Ni alloys. Acta Mater, 2005, 53: 759–764
4 Mooij JH. Electrical conduction in concentrated disordered transition metal alloys. Phys Stat Sol (a), 1973, 17: 521–530
5 Cochrane RW, Harris R, Ström-Olson JO, *et al.* Structural manifestations in amorphous alloys: resistance minima. Phys Rev Lett, 1975, 35: 676–679
6 Mizutani U, Yoshino K. Formation and low-temperature electronic properties of liquid-quenched Ag-Cu-X (X=Mg, Si, Sn and Sb) metallic glasses. J Phys F-Met Phys, 1984, 14: 1179–1192
7 Chen AB, Weisz G, Sher A. Temperature dependence of the electron density of states and dc electrical resistivity of disordered binary alloys. Phys Rev B, 1972, 5: 2897–2924
8 Anderson PW. Absence of diffusion in certain random lattices. Phys Rev, 1958, 109: 1492–1505
9 Singh D, Singh D, Srivastava ON, *et al.* Microstructural effect on the low temperature transport properties of Ce–Al (Ga) metallic glasses. Scripta Mater, 2016, 118: 24–28
10 Altshuler BL, Aronov AG. Electron-electorn interaction in disordered conductors. In: Efros AL, Pollak M (Eds.). New York: Elsevier Science Publishing Company, Inc., 1985, pp 4
11 Stillinger FH. A topographic view of supercooled liquids and glass formation. Science, 1995, 267: 1935–1939
12 Luo P, Wen P, Bai HY, *et al.* Relaxation decoupling in metallic glasses at low temperatures. Phys Rev Lett, 2017, 118: 225901
13 Zhu F, Nguyen HK, Song SX, *et al.* Intrinsic correlation between β-relaxation and spatial heterogeneity in a metallic glass. Nat Commun, 2016, 7: 11516
14 Debenedetti PG, Stillinger FH. Supercooled liquids and the glass transition. Nature, 2001, 410: 259–267
15 Adam G, Gibbs JH. On the temperature dependence of cooperative relaxation properties in glass-forming liquids. J Chem Phys, 1965, 43: 139–146
16 Stevenson JD, Schmalian J, Wolynes PG. The shapes of cooperatively rearranging regions in glass-forming liquids. Nat Phys, 2006, 2: 268–274
17 Yeh JW, Chen SK, Lin SJ, *et al.* Nanostructured high-entropy alloys with multiple principal elements: novel alloy design concepts and outcomes. Adv Eng Mater, 2004, 6: 299–303
18 Zhang Y, Zuo TT, Tang Z, *et al.* Microstructures and properties of high-entropy alloys. Prog Mater Sci, 2014, 61: 1–93
19 Zhao K, Xia XX, Bai HY, *et al.* Room temperature homogeneous flow in a bulk metallic glass with low glass transition temperature. Appl Phys Lett, 2011, 98: 141913
20 Zhang W, Liaw PK, Zhang Y. Science and technology in high-entropy alloys. Sci China Mater, 2018, 61: 2–22
21 Zhao S, Wang H, Gu J, *et al.* High strain rate sensitivity of hardness in Ti-Zr-Hf-Be-(Cu/Ni) high entropy bulk metallic glasses. J Alloys Compd, 2018, 742: 312–317
22 Wang X, Dai W, Zhang M, *et al.* Thermoplastic micro-formability

of TiZrHfNiCuBe high entropy metallic glass. J Mater Sci Tech, 2018, 34: 2006–2013
23 Cheng CY, Yeh JW. High-entropy BNbTaTiZr thin film with excellent thermal stability of amorphous structure and its electrical properties. Mater Lett, 2016, 185: 456–459
24 Lu ZP, Bei H, Wu Y, *et al.* Oxygen effects on plastic deformation of a Zr-based bulk metallic glass. Appl Phys Lett, 2008, 92: 011915
25 Li HX, Gao JE, Jiao ZB, *et al.* Glass-forming ability enhanced by proper additions of oxygen in a Fe-based bulk metallic glass. Appl Phys Lett, 2009, 95: 161905
26 Gerstenberg D, Calbick CJ. Effects of nitrogen, methane, and oxygen on structure and electrical properties of thin tantalum films. J Appl Phys, 1964, 35: 402–407
27 Liu W, Zhang H, Shi JA, *et al.* A room-temperature magnetic semiconductor from a ferromagnetic metallic glass. Nat Commun, 2016, 7: 13497
28 Mueller R, Agyeman K, Tsuei CC. Negative-temperature coefficients of electrical resistivity in amorphous La-based alloys. Phys Rev B, 1980, 22: 2665–2669
29 Lee PA, Ramakrishnan TV. Disordered electronic systems. Rev Mod Phys, 1985, 57: 287–337
30 Manyala N, Sidis Y, DiTusa JF, *et al.* Magnetoresistance from quantum interference effects in ferromagnets. Nature, 2000, 404: 581–584
31 Gale WF, Totemeir TC. Smithells Metals Reference Book, 8th Edition. (Ch. 8: Table 8.8e). New York: Elsevier Ltd. 2003

Acknowledgements This work was supported by Qian Xuesen Laboratory of Space Technology and the National Natural Science Foundation of China (51471091).

Author contributions Zhao S prepared the manuscript under the supervision of Yao KF, Chen N, and Wang WH. Wang P, Cheng X and Zhang Q revised the manuscript. Zhang Y and Wen Z conducted the PPMS experiments. All authors contributed to the general discussion.

Conflict of interest The authors delare no conflict of intrest.

Shaofan Zhao obtained his PhD in materials science and engineering from Tsinghua University in 2015. Then he worked as a postdoctoral associate in the Department of Mechanical Engineering and Materials Science, Yale University for one and half years. His research interest focuses on Ti-based bulk metallic glasses (BMGs) and high-entropy alloys. Now he is an assistant professor in Wei-Hua Wang's research group at Qian Xuesen Laboratory of Space Technology, and this reseach group is trying to increase the space engineering usefulness of BMGs.

Na Chen received her PhD degree in materials science and engineering from Tsinghua University in 2008. She was a Research Associate in the World Premier International Research Center Initiative-Advanced Institute for Materials Research (WPI-AIMR), Tohoku University of Japan in 2008, where she became an Assistant Professor in 2010. From 2011 to 2012, she was a Visiting Scientist in the Institute of Nanotechnology, Karlsruhe Institute of Technology, Karlsruhe, Germany. In 2013, she became an Associate Professor in the School of Materials Science and Engineering, Tsinghua University. Her current research interests include the design and synthesis of advanced non-equilibrium metals and their derivatives.

Ti-Zr-Hf-Cu-Ni高熵非晶合金薄膜中掺氧诱导的低温异常电输运行为

赵少凡[1*], 王鹏飞[1], 程祥[1], 张盈琪[2], 温卓群[1], 张琪[1], 姚可夫[2], 陈娜[2*], 汪卫华[3]

摘要 低温电输运特性是非晶态材料理论研究中的关键问题. 通过在Ti-Zr-Hf-Cu-Ni高熵非晶合金薄膜材料中掺入氧, 可以诱导其在低温下显示出异常的电输运行为. 低于8 K时, 掺氧高熵非晶合金薄膜的电阻率分别与温度和外加磁场强度的1/2次方即$T^{1/2}$和$H^{1/2}$呈线性关系. 研究表明, 氧的掺入增强了高熵非晶合金薄膜中电子-电子间的库伦作用和电子自旋之间的交互作用, 从而导致含氧高熵非晶合金薄膜的低温异常磁电输运行为. 因此我们可通过对高熵非晶合金材料掺氧实现对该材料低温导电性能的调控.

